A review on the instantaneous angular speed estimation with application to an aircraft engine

Edgar F. Sierra-Alonso [1,2], Jerome Antoni [1], German Castellanos-Dominguez[2]

[1] Laboratoire Vibrations Acoustique, Univ Lyon, INSA-Lyon,
LVA EA677, F-69621, Villeurbanne, France,
edgar-felipe.sierra-alonso@insa-lyon.fr
[2] Signal Processing and Recognition Group, Universidad Nacional de Colombia,
Km 9 way to magdalena, Manizales Caldas, Colombia

Abstract

This work presents a short review of the state-of-the-art on the subject of Instantaneous Angular Speed (IAS) estimation. Departing from the definition of IAS as a fundamental frequency of a superposition of sinusoids, convolved with a transfer function plus noise. With this in mind, the discussed methodologies are restricted to the ones for IF estimation on multicomponent signals, more precisely, to the fundamental frequency estimation ones. For an experimental validation, we study three measured signals, a vibration signal from a test rig affected by a resonance frequency, a vibration and an acoustic signal from an aircraft engine. As a conclusion, with an expert initial examination of the signal and a priori knowledge of the machine, the IAS can be accurately estimated from the vibration signal in both cases, in contrast, the IAS estimation using the acoustic signal needs to be improved.

1 Introduction

The Instantaneous Angular Speed (IAS) alongside the vibroacoustic data is one of the most important parameters to measure in condition monitoring. For instance, in the case of bearing failure identification, the frequencies of the failure are a function of the IAS, making impossible to identify a failure without this parameter [1]. The IAS is usually available after processing the tachometer signal. However, the speed measurement through the tachometer signal is sensitive to some disturbances, like lost samples, or artifacts in the measurement [2]. Alternatively, the IAS can be extracted directly from the vibration signal, being this the most difficult situation. Due to the multicomponent nature of the signal, where different families of harmonics may coexist, alongside with the interaction between the orders and the structural resonances of the machine. Besides the above-mentioned problems, it is usual to deal with a low Signal to Noise Ratio (SNR) where noise comprises any component in the signal which is not of direct interest for the analysis [3].

Despite the growing interest in IAS estimation from vibroacoustic signals over the last few years evidenced in the special issue [4], there are no reviews dedicated to IAS estimation. The reason lies in the tight relationship between IAS and Instantaneous Frequency (IF). Being the IAS usually estimated relating a particular set of IF laws of a vibration signal to the physical phenomenon with the help of an expert initial visual examination of the signal and/or the kinematics of the machine [3, 5–7].

To not to repeat the work of the reviews on IF estimation for general digital signal processing like [8–10]. This work proposes to review the definition of the IAS, departing from the traditional IF definition of telecommunications. Where it is defined a frequency modulation as a variation of the instantaneous frequency of a carrier wave [9], arriving at the definition of the IAS as the time-varying fundamental frequency of a superposition of harmonically related sinusoids, convolved with a transfer function plus Additive White Gaussian Noise (AWGN). After this definition, the problem of IAS estimation is narrowed to a fundamental frequency estimation one. In consequence, some representative works in the state-of-the-art on that specific subject are discussed and arranged into parametric and non-parametric approaches.

Three challenging signals are used to validate the definition of the IAS reviewed in this work, a vibration signal from a test rig affected by a resonance under a run-up test, a vibration signal (available as supplementary material in [11]) and an acoustic signal both from an aircraft engine. The spectrogram is selected as the main tool to analyze the signals mentioned above, due to it is the core for most of the time-frequency approaches, as studied in the review [8]. Alongside with the spectrogram, the short-time-scale transform proposed in [12], it is applied to the aircraft engine signals and compared with a signal of reference obtained from the tachometer signal.

The agenda of this paper is the following: it is reviewed in Section 2 the definition of the IAS departing from the IF of a monocomponent signal. In the Section 3 it is discussed the most representative and latest IF estimation methods on multicomponent signals, to arrive at the fundamental frequency estimation ones applied to rotating machines, in the Section 4 it is studied three challenging signals from a test rig and an aircraft engine.

2 Instantaneous Angular Speed: A brief theoretical background

The aim of this section is to define the Instantaneous Angular Speed (IAS) as a fundamental frequency of a multicomponent signal, departing from the classical definition of the IF used in the theory of frequency modulation. Also, to discuss some limitations of the definition of the IF.

2.1 Instantaneous Frequency

Before to introduce the definition of IAS, it is necessary to define the Instantaneous Frequency (IF). Let us depart from the definitions used in the work [9]. Be $x(t)$ an amplitude modulated and frequency modulated (AM-FM) real valued signal:

$$x(t) = A(t)\cos\left[2\pi\int_0^t f_0(\tau)d\tau + \theta\right] \tag{1}$$

where the integral is defined for each t value in $[0,T]$ the time domain , $A(t)$ is a time varying amplitude, θ is a constant representing an initial phase, and $f_0(t)$ is the IF, which is related with the phase $\phi_0(t)$ by means of the fundamental theorem of calculus as:

$$f_0(t) = \frac{1}{2\pi}\frac{d\phi_0(t)}{dt} \tag{2}$$

Nevertheless, it is often convenient to consider an analytic signal[1], for instance, the analytic signal allows the definition of the Gabor's central moments of frequency of the signal (view [9]). Therefore, this initial definition is extended for $z(t)$ the analytic signal, where $z(t)$ is constructed from $x(t)$ using $\mathscr{H}\{\cdot\}$, i.e, the Hilbert Transform (HT) as following:

$$z(t) = x(t) + j\mathscr{H}\{x(t)\} \tag{3}$$
$$= A(t)[\cos\phi_0(t) + \mathscr{H}\{\cos\phi_0(t)\}] \tag{4}$$
$$= A(t)e^{j\phi_0(t)} \tag{5}$$

where $j=\sqrt{-1}$. The IF $f_0(t)$ is retrieved from the analytic signal $z(t)$, using the derivative of its argument $\arg z(t)$, similarly as in the previous Eq. (2) it is formally written as:

$$f_0(t) = \frac{1}{2\pi}\frac{d\arg z(t)}{dt} \tag{6}$$

The definition of the IF departing from a real signal comes with restrictions that worth mentioning: to arrive from Eq. (3) to Eq. (4) it is necessary to apply the Bedrosian theorem. However, this theorem does not allow us in a general framework to arrive at Eq. (5), an example of this statement and a subsequent study can be found in [13]. Consequently, the definition in Eq. (6) in a general framework it is not a relationship of equality. A recent work that takes into account the study of [13]. It is [14], where the authors compare

[1] an analytic signal is a complex signal, whose Fourier Transform has non-negative frequencies.

different IF estimation algorithms, and they arrive at a conclusion, that even when it is not possible to have a perfect in-quadrature component using the HT to arrive at the Eq. (5), it is still the most accurate mathematical tool to compute the IF. More precisely the most accurate it is the Normalized Hilbert Transform (NHT), which consist of using the Eq. (6) in a monocomponent pure phase signal, i.e., a signal whose amplitude is constant (the unity). Therefore, the critical step is to pre-process the measured signal to ensure a monocomponent pure phase signal.

2.2 Instantaneous Angular Speed

The IAS is an IF law, but it is not possible to define it directly from the measurement of $x(t)$. Due to the IAS is the fundamental IF law of a harmonic sum, convoluted with the transfer function $h(t)$ of the structure, plus the measurement noise $\eta(t)$. Which for simplicity it is usually assumed to be Additive White Gaussian Noise (AWGN), i.e., $\eta(t) \sim \mathcal{N}(0, \sigma_\eta^2)$, in mathematical terms the vibration signal $x(t)$ is expressed as:

$$x(t) = h(t) * d(t) + \eta(t) \tag{7}$$

where $(\cdot * \cdot)$ is the convolution operator between two functions, $d(t) = \sum_{k=1}^{K} x_k(t)$ is a deterministic multi-component AM-FM function, where each $x_k(t)$ and $\phi_k(t)$ are defined as follows:

$$\begin{aligned} x_k(t) &= A_k(t)\cos 2\pi\phi_k(t) \\ \phi_k(t) &= \int_0^t f_k(\tau)d\tau + \theta_k \end{aligned} \tag{8}$$

the set of IFs $\{f_k\}_{k=1}^{K}$, it is assumed to be harmonically related with the IAS $f_0(t)$, so each IF is written in terms of the IAS as $f_k(t) = \alpha_k f_0(t)$ for α_k a real scalar, it worth nothing to mention that in the case of only one harmonic family α_k is a natural number.

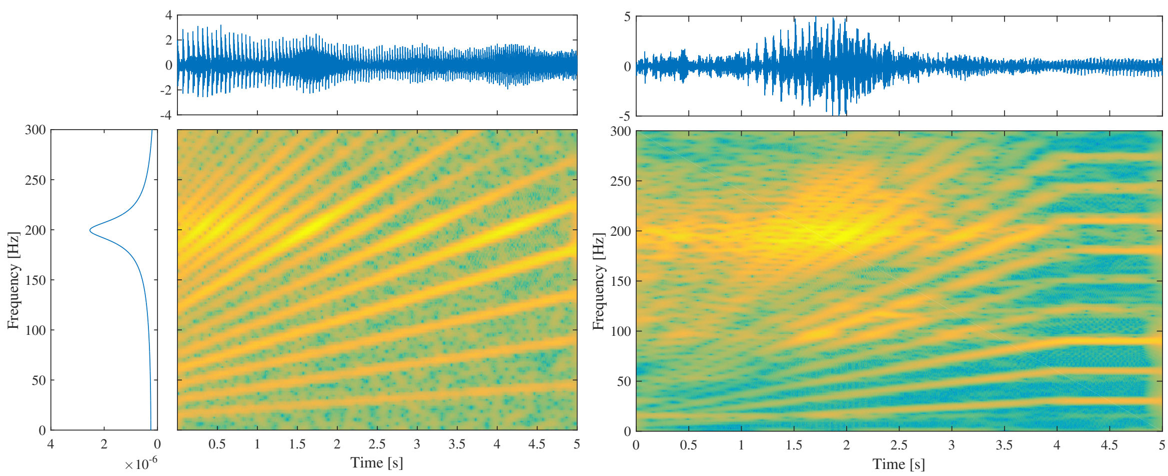

(a) Transfer function in frequency domain (left), signal in time (top), and spectogram in the (center).

(b) Signal in time (top) and spectrogram of the test-rig signal (bottom).

Figure 1 – An example of a numerical signal generated using the model of the Eq. (7) is shown in Fig. 1a, and in Fig. 1b a real vibration signal from a test rig (for the description of the test rig please refer to [15]).

To give an illustration of the phenomenon modeled by the Eqs. (7) and (8). The Fig. 1 shows a numerical and a real vibration signal, both affected by a resonance frequency located around 200Hz. The Fig. 1b shows a 5 seconds run-up test in a test rig. The run-up test goes from a steady state to maximum operational speed 1800RPM or 30Hz at a sampling frequency of 20kHz. The numerical signal inspired by the test-rig measurement is shown in Fig. 1a. It has a sampling frequency of 1024Hz a duration of 5 seconds, the theoretical IAS is a chirp that goes from 15Hz to 30Hz, and it has Signal to Noise ratio (SNR) of 6dB. For comparison purposes, it is only displayed the frequencies comprised within the interval $[0, 310]$Hz, where the resonance frequency is located. It should be noticed that all the spectrograms in this work are going to be shown with the energy in logarithmic scale[2], only for visualization purposes.

Given the model in Eq. (7), the intuitive definition of the IAS is using the Eq. (6) on the argument of $z_1(t)$ the analitic signal of $x_1(t)$. However, as the IAS is a fundamental frequency to add accuracy to the estimation, it is natural to think on an "averaged" estimation simultaneously involving all the harmonics of the IAS. Recently, in [11] a harmonic demodulation estimator for the IAS is defined as follows:

$$\hat{f}_1(t) = \frac{\sum_{k=1}^{K} \Im\{\dot{z}_k(t) z_k(t)^*\}}{\sum_{k=1}^{K} \alpha_k |z_k(n)|^2} \tag{9}$$

where $\Im\{\cdot\}$ represents the imaginary part of a complex number, and $\dot{z}_k(t)$ is the time derivative of $z_k(t)$, which is constructed from $x_k(t)$ using the Eq. (3). Nevertheless, the demodulation method in Eq. (9) requires estimating the components $\{x_k(t)\}_{k=1}^{K}$ from the vibration signal. Which in a general framework it is not a trivial task because in practice the noise is not AWGN. Furthermore, any components that do not fit into the model, like crossed components have to be considered as noise [3].

3 IF estimation on multicomponent signals

The problem of estimating the instantaneous components of a multicomponent signal it is not new, yet it remains challenging. As stated by [8] "after more than three decades of development, the problem of estimating multicomponent signals is still open for research". The most recent technique designed for the study of multicomponent signals is empirical mode decomposition (EMD). EMD has become a popular tool to separate a signal, due to it ensures an additive representation of the signal into a finite set of Intrinsic Mode Functions (IMF), a function assumed to be monocomponent [16]. One of many application of EMD is fault detection in rotating machines. An entire review on the subject can be found in [17]. Even when EMD has proven its usefulness, it is not characterized as a filter. Consequently, it remains undetermined the separability of the components of a signal using EMD. However, there are some advances on the subject, for instance, in [18] it is established that EMD presents a quasi-dyadic filter structure when broadband noise is considered, and in [19] the authors conclude that EMD acts as an almost linear filter for the following two tones separation case:

$$x(t; a, f) = \cos 2\pi t + a\cos(2\pi f t + \theta) \tag{10}$$

where the term $\cos 2\pi t$ is the higher frequency component and $a\cos(2\pi f t + \theta)$ the low frequency component. One conclusion of [19] that has to be mentioned is that EMD can never retrieve the two tones when $a^2 f > 1$ for a normalized frequency axis, i.e., $f \in [0, 1]$. Later, with the spirit of EMD, a synchrosqueezed improvement of the wavelet transform was introduced in [20], where the authors replaced the empirical notion of IMF, formally defining a class of well-separated functions termed intrinsic mode type components (IMT). The main result is that the IMT components can be identified and characterized using synchrosqueezing. The problem in our case is that, in general, there are not well-separated components. As it is the case of study in [21], where it is proposed a generalized synchrosqueezing transform (GST), that introduces a demodulation step using an initial estimation of the IF law of interest before the application of the synchrosqueezed wavelet transform, improving the "readability" of the Time Frequency Representation (TFR).

In the state-of-the-art, some techniques also use an initial guess of the IF of interest to improve the TFR of a multicomponent signal. For instance, in [22–25] it is also obtained high-resolution IF ridges even in the presence of crossed spectral components, using improved TFR representations based on different polynomial parametrization of the STFT; where the polynomial approximates the phase of interest ($\phi_0(t)$ in our case). The aforementioned works uses different enhanced TFRs, for instance, In [23] it is used the Polynomial Chirplet transform (PCT), in [22] the spline-kernelled Chirplet Transform (SCT), and in [24, 25] the Local Polynomial Fourier Transform (LPFT). The differences and similarities between the TFRs are not a part of the scope of the present work. However, due to the importance and renewed interest of the LPFT evidenced in the review [25], it is mandatory to introduce at least its definition:

[2] an spectrogram with its energy in logarithmic scale is defined as $\log(|\mathrm{STFT(t,f)}|^2)$ where $\mathrm{STFT(t,f)}$ represents the Short-Time Fourier Transform (STFT) and $|\cdot|$ the modulus.

$$\mathrm{LPFT}(x;t,\boldsymbol{\omega}) = \int x(t+\tau)w(\tau)e^{-j\Phi(\tau,\boldsymbol{\omega})}d\tau \tag{11}$$

where $w(\tau)$ is a window function, i.e. a function centered at $t=\tau$ such that $\int_{-\infty}^{\infty} w(\tau)d\tau = 1$, the parametrized phase is $\Phi(\tau,\boldsymbol{\omega}) := \sum_{m=0}^{M-1} \omega_m \tau^{m+1}/(m+1)!$, and $\boldsymbol{\omega}$ is the set of parameters defined as $\boldsymbol{\omega} := [\omega_0, \omega_1, \omega_2, \ldots, \omega_{M-1}]$. The most important fact about the LPFT is that it is a natural extension of the STFT. Furthermore, the linearity of the STFT is inherited by the LPFT.

Returning to our particular problem of IAS estimation, it is not only required to deal with the presence of crossed components and close harmonics. The interaction with the transfer function of the structure $h(t)$ has to be considered as well as a low SNR, a common restriction for acoustic signals. Consequently, if the IF law of interest (the IAS) pass by a resonance frequency a contaminated IF law will be obtained disregard the estimation methodology used. The most direct solution will be to track a harmonic of the IAS such that it is not affected by the resonance and afterwards to correct the scale to obtain the IAS as $f_0(t) = \alpha_k^{-1} f_k(t)$. Nevertheless, in the worst case scenario, i.e., if such $f_k(t)$ does not exist, a reasonable approach is to extract/model simultaneously all the harmonically related components $\{f_k(t)\}_{k=1}^{K}$. To do so approaches in the state-of-the-art based on the fundamental frequency estimation should be considered.

3.1 Fundamental frequency estimation: parametric approaches

In the literature, the estimation of a time-varying fundamental frequency is commonly addressed in a parametric manner using a modeling[3] of the Eq. (7). For instance [27] proposes a comparison between three adaptive estimators: Extended Kalman Filter (EKF), Unscented Kalman Filer (UKF) and Particle Filter (PF), to track simultaneously the instantaneous amplitude and phase of an AM-FM signal. As a conclusion, the PF is the most reliable estimator, and if the signal is perfectly described by the model, the EKF has the best performance/complexity trade-off among all the considered estimators.

In the particular field of digital signal processing applied to mechanical systems, the authors in [28] proposed the use of the EKF to process a vibration signal from a ship drive line. However, the use of the EKF comes with some practical limitations, for instance, it is required to have an accurate model of the measured signal. That model requires an a priori identification of the spectral components present in the measured signal, which translates into a different modeling per machine. Addressing this limitation, [6] introduced a more general approach. It was abandoned the assumption of a fundamental frequency, proposing a divide and conquer approach, i.e., to model through the EKF and to filter each spectral component independently, where, to filter in this sentence indicates the use of a pass-band-filtering for the spectral components of interest. It should be remarked that in [6] it is addressed both problems, the spectral components identification, and the initialization of the EKF making use of the Spectral Kurtosis, unfortunately, the case of large variations in the speed, like a run-up test, it is not a subject of study in [6].

Initially one can wrongly assume that the three works mentioned above [6,27,28] attempt to solve the same problem with the same tool (adaptive filters). However, the main difference is the proposed model, mainly in the case of the work of [6], which can not be classified as a purely fundamental frequency estimation approach as it estimates the IF of each spectral component individually. In the future, it will be interesting to have a comparison between the three works.

3.2 Fundamental frequency estimation: non-parametric approaches

An entire non-parametric approach that makes no use of a priori knowledge is proposed in [12], where it is assumed that given two windowed segments[4] $x(t;\tau_i)$ and $x(t;\tau_{i+1})$ of the vibration signal $x(t)$ can be modeled as two independent vibration signals at different constant speeds v_i, v_{i+1}, where $x(t;\tau_{i+1})$ can be rewritten as

[3] the model for a Kalman Filter has two parts: a state space equation that encodes the dynamics of the system, and a measure equation that relates the dynamics of the system with the measurement $x(t)$, for a detailed explanation, please refer to [26].

[4] given a signal $x(t)$ and a window function $w(t)$ the i-th segment of a signal is defined as $x(t;\tau_i) = x(t)w(t-\tau_i)$ for a fixed real value τ_i of an increasing sequence $\{\tau_i\}_{i\in I}$.

a time-warped version of $x(t;\tau_i)$ which is $x(t;\tau_{i+1}) \approx x(a_{i,i+1}(t-t_0);\tau_i) + \eta(t)$. To identify the time-warping scale $a_{i,i+1}$ it is used the scale transform, defined as:

$$D_x(w) = \frac{1}{\sqrt{2\pi}} \int_0^\infty x(t) \frac{e^{-jw\ln t}}{\sqrt{t}} dt \tag{12}$$

where w stands for the scale variable of the transform. The key property of the scale transform is the scale invariance, i.e. if $x(t;\tau_{i+1})$ can be expressed as an energy normalized time-warping of $x(t;\tau_i)$, which is $x(t;\tau_{i+1}) = \sqrt{a_{i,i+1}}x(a_{i,i+1}t;\tau_i)$ then $D_{x(t;\tau_{i+1})}(w) = D_{x(t;\tau_i)}(w)e^{jw\ln a_{i,i+1}}$. Consequently, per each scale w the time-warping scale $a_{i,i+1}$ can be founded using the phase difference between $D_{x(t;\tau_i)}(w)$ and $D_{x(t;\tau_{i+1})}(w)$, defined as $\Delta\phi_{i,i+1}(w) = \phi_{D_{x(t;\tau_{i+1})}}(w) - \phi_{D_{x(t;\tau_i)}}(w) = w\ln a_{i,i+1}$. As each phase difference $\Delta\phi_{i,i+1}(w)$ depends on the scale variable w, to obtain a robust estimation the authors considered a linear regression on the scale variable w, for more details about the estimation of the time-warping scale $a_{i,i+1}$ and the short-time formulation please refer to [12].

Another interesting work that also models the variation of the rotational speed as a time-warping function is [29], where the signal under variable speed is modeled as a deformed stationary complex random Gaussian signal. Consequently, it can be characterized by its covariance matrix, leading to the formulation of a maximum likelihood estimator for the IAS. Nevertheless, the main contribution of [29] it is not the extraction of the IAS itself. It is the reformulation/formalization of the IAS estimation problem in stochastic terms, where the "deterministic" part of the signal (the IAS) deforms a pure complex Gaussian random signal. In words of the authors, it is introduced the "*timbre x dynamics* models: models in which a stationary random signal (whose power spectrum is interpreted as timbre) is modified by some nonlinear function, which encodes the dynamics of some underlying systems."

The aforementioned works [12, 29] do not require any a priori knowledge of the machine. However, if we have access to the kinematics of the machine that knowledge will dramatically improve the estimation accuracy of the IAS. As in [3], where, the authors propose a methodology named multiorder probabilistic approach (MOPA), that uses all the a priori knowledge about the kinematics, to fusion all the spectral components related to the gear mesh frequencies and its harmonics, to finally obtain the IAS after a smoothing operation. MOPA was applied to a challenging signal recorded from the gearbox of a wind turbine, showing a remarkable performance in terms of a relative error below 0.4% with respect to IAS estimated processing the tachometer signal.

A final remark about the approaches considered in [12, 29], is that they are not are not fundamental frequency approaches in a strict sense, i.e., they do estimate an IF that is related with the IF law that generates a harmonic family. However, such IF may not correspond to the IF law of a spectral component of the signal. In mathematical terms the tracked IF $\hat{f}_0(t) = kf_0(t)$, for a certain scale $k \in \mathbb{R}$. Furthermore, the authors in [12] do not use the term IAS. Instead, they introduce the term Instantaneous Speed Relative Fluctuation (ISRF), the definition and an application of the estimation of the ISRF will be given in the next section.

4 Application to the acoustic signal from an aircraft engine

The aim of this section is to motivate further study on IAS estimation using acoustic signals, rather than compare the different approaches named in the previous Section 3. To do so, it is only applied two exemplary IAS estimation techniques to the vibration and acoustic signals from an aircraft engine, and to a challenging test rig signal with a resonance at 200Hz (view Fig. 1b). The two techniques chosen are: a robust Time Frequency Distribution (TFD) maximum tracking, and the scale transform (view Eq. (12)) based algorithm proposed by [12].

4.1 Description of the aircraft engine and recorded data

The data was acquired during a ground test on a civil aircraft engine. The Fig. 2 gives a general overview of the engine with the damaged bearings and the sensors locations. The engine has two main shafts and an accessory gearbox with pieces of equipment such as pumps, filters, alternators, and starter. The accessory gearbox is linked to the high-pressure shaft HP by a radial drive shaft and a horizontal drive shaft. As the

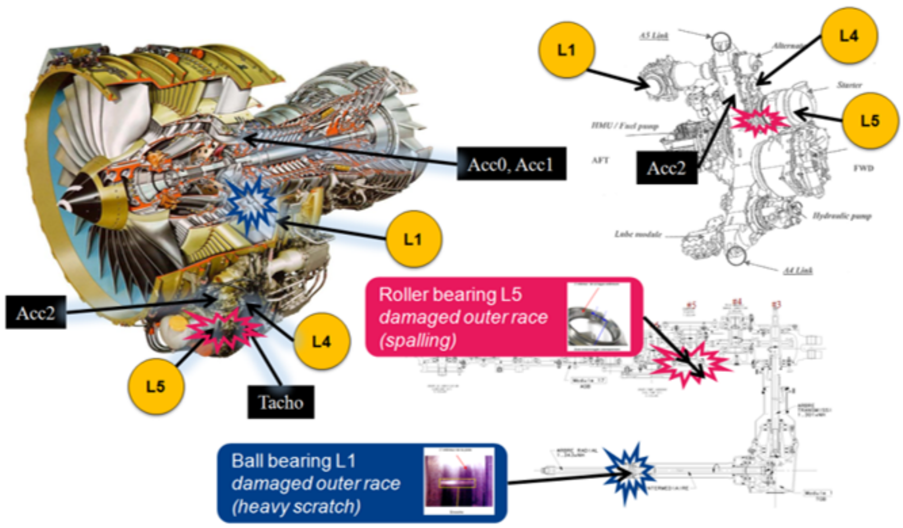

Figure 2 – General overview of the engine and the accessory gearbox. Shafts (L1-L5) are identified by labels in amber color (image taken from [11]).

records will only be used for the IAS estimation, it is not going to be proportioned here detailed information about the kinematics and the bearing faults frequencies, if necessary, please refer to [11].

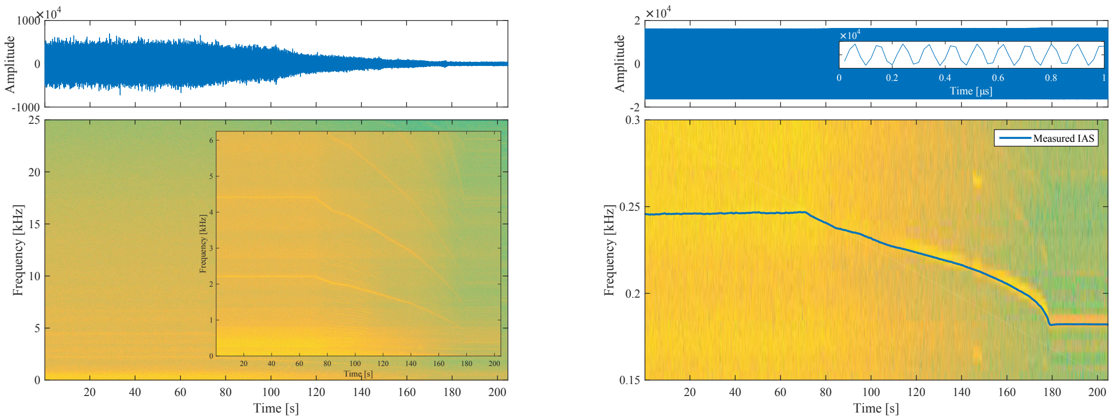

(a) Signal in time (top), and spectrogram (bottom), with a zoom on the bandwidth $[0, 6.25]\mathtt{kHz}$.

(b) Tachometer signal and a zoom in the time interval $[0, 1]\mu\mathtt{s}$ (top), the estimated IAS from the tachometer measurement with the spectrogram of the acoustic signal (bottom).

Figure 3 – Raw acoustic signal and its spectrogram (Fig. 3a) raw tachometer signal and the estimated IAS from the tachometer superposed on the spectrgram of the acoustic signal (Fig. 3b).

For an initial visual inspection of the acoustic signal, the Fig. 3b shows the raw signal sampled at $50\mathtt{kHz}$ and its spectrogram. Nevertheless, in such wide range of frequencies, it is not possible to accurate visualize the spectral components. For such reason, the Fig. 3a shows also a zoom in the frequency range $[0, 6.25]\mathtt{kHz}$, where two main IF laws are identifiable starting at $2.2\mathtt{kHz}$ and $4.4\mathtt{kHz}$. To relate the spectral components with the IAS, the Fig. 3b shows the measured IAS from the tachometer signal using as background the spectrogram of the raw signal in the frequency range $[0.15, 0.3]\mathtt{kHz}$. From the visual inspection of the Fig. 3a can be concluded, that the most direct approach will be to track one of the highest energy components, assuming that it is a *harmonic of the IAS*.

After the visualization, it is inferred that the minimum pre-processes to deal with the acoustic signal (in Fig. 3a) must be a low-pass filter and a posterior down-sampling, to take into account only the frequencies bellow $6.25\mathtt{kHz}$. Similarly, for the vibration signal of the test rig in the Fig. 1b, as the resonance frequency is located around $200\mathtt{Hz}$ it is considered only the frequencies bellow $310\mathtt{Hz}$. The parameters for the computation of the STFT are a Hamming window of 256 and 4096 bins, for the test rig and aircraft engine signals respectively, which in time it is approximately $0.5\mathrm{s}$. For the frequency resolution, it is used the same amount of frequency bins as the length of the time window. As it is expected for the IAS to have slow variations and to use the minimum possible computational resources the window overlap selected was of 70%. For consistency, all the Short-Time computations using these signals will have the same parameters.

Before to continue with the IAS estimation, it should be mentioned that the IAS was already successfully estimated for this aircraft engine using only the vibration signal, the entire study alongside with the accelerometers and tachometer records can be found in [11]. As the data is publicly available, the IAS will be firstly estimated on the vibration signal only to use it as a reference point to process the acoustic record. To not to lose the scope of this paper, the main similarities or differences between the acoustic and vibration signals regarding IAS estimation will be studied only in a qualitative manner.

4.2 IAS estimation: Time Frequency Distribution

To introduce the IF estimation algorithm it is necessary to define the STFT, which is defined from the Eq. (11), as $\mathrm{STFT}(t,f) = \mathrm{LPFT}(t,\boldsymbol{\omega})$ for $M = 1$, where for this particular case $\boldsymbol{\omega} = \omega_0$, being ω_0 the frequency variable in radians[5]. With this definition in mind and taking into account that the spectrogram $|\mathrm{STFT}(t,f)|^2$ can be assumed to be a Time Frequency Distribution (TFD), the IF of a monocomponent signal can be retrieved from a TFD using the following expression:

$$\hat{f}_0(t) = \frac{\int_0^\infty f|\mathrm{STFT}(t,f)|^2 df}{\int_0^\infty |\mathrm{STFT}(t,f)|^2 df} \tag{13}$$

But as the case of study is a multicomponent signal, an IF estimation $\hat{f}_k(t_i)$ of an IF law of interest $f_k(t)$, cannot be defined from a TFD using the Eq. (13). However, it can be estimated, where the estimated IF law $\hat{f}_k(t_i)$ is the frequency associated with the largest peak in an adaptive search interval $[f_c(t_i) - \delta, f_c(t_i) + \delta]\mathrm{Hz}$ of bandwidth 2δ, where the closed interval is centered at $f_c(t_i)$, at the time instant t_i. As the IF changes each time instant the search interval has to change also, therefore, $f_c(t_{i+1})$ is defined using a recursion that takes into account the current estimation $\hat{f}_k(t_i)$ and the current central frequency $f_c(t_i)$ of the search interval, as follows:

$$f_c(t_{i+1}) = \beta f_c(t_i) + (1-\beta)\hat{f}_k(t_i) \tag{14}$$

where the variable $\beta \in [0,1]$ represents a forgetting factor, i.e, if $\beta = 0$ the next central frequency $f_c(t_{i+1})$ will be $\hat{f}_k(t_i)$, the IF estimated at the current time instant, and if $\beta = 1$ then $f_c(t_{i+1}) = f_c(t_i)$.

The parameters used in Fig. 4 for the tracking algorithm in Eq. (14) are: the forgetting factor β, the bandwidth for the search interval δ, and the initial central frequency $f_c(t_0)$. The forgetting factor is heuristically fixed at 0.7, as the change between time instants is expected to be smooth. The choice of the bandwidth it is not crucial, similar results are obtained for $\delta \in [5,10] \subset \mathbb{N}$ bins. The critical parameter is the initial central frequency, which has to be close to the localization of the desired IF to be tracked at the initial time instant.

As results, the Fig. 4 shows in red the estimated IF laws for all the considered signals. The top row shows the extracted IF laws for the vibration signals, and the bottom row the tracked IF laws for the acoustic signal. For the test rig with the resonance the Fig. 4c shows the IF laws corresponding to the harmonics x1, x3, x5, where the major error in the estimation is seen in the firsts $0.5\mathrm{s}$, caused by the presence of close orders.

The Figs. 4a and 4b show the tracked IF laws for the *vibration signal* of the aircraft engine. The Fig. 4a shows the highest energy component located at $2.2\mathrm{kHz}$. To attempt to establish the origin of such spectral component, the Fig. 4b shows a zoom in of the spectrogram. Where the fourth harmonic of the IAS located around $1\mathrm{kHz}$ is highlighted in red line, and above it, the $2.2\mathrm{kHz}$ component which crosses the IAS harmonics making even more difficult the labor of the tracking algorithm based on TFD. However, as expected the dominant spectral components are governed by the IAS, in consequence, the Fig. 4a shows an undeniable harmonic of the IAS, from which the IAS can be obtained after a correction of the scale of the tracked IF law.

The Figs. 4d and 4e show in red the tracked IF laws for the *acoustic signal*. As it was expected the IAS estimation is a more challenging task using the acoustic signal, particularly in this case, due to the IAS and its harmonics are masked by the dominant harmonic family of the $2.2\mathrm{kHz}$ component. Nevertheless, the IAS

[5]the variable ω_0 represents ω in the standard definition of the STFT, the sub-index 0 in this case does not indicate a fundamental frequency.

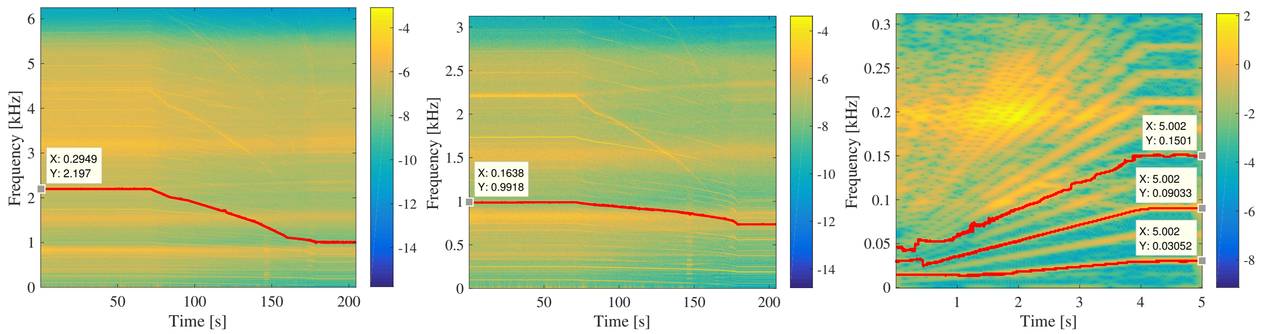

(a) Tracked IF associated with highest energy component.

(b) Fourth IAS harmonic tracked after a visual examination of the spectrogram.

(c) Spectrogram and IFs corresponding to the harmonics x1, x3, x5.

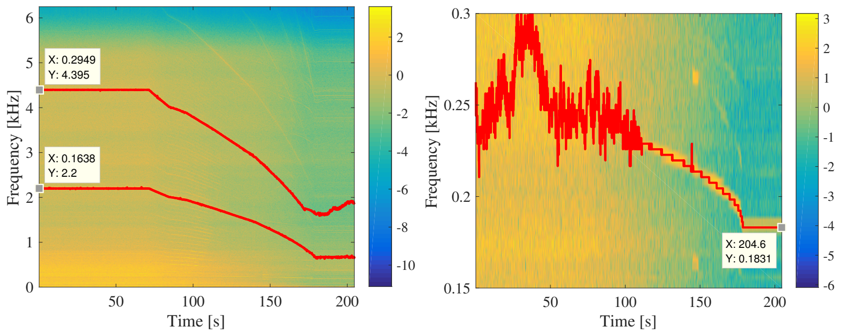

(d) Spectrogram, the highest energy IF law, and its second harmonic.

(e) Spectrogram, the IAS tracked using 220Hz as initial central frequency.

Figure 4 – IF laws estimated (in red), using as initial central frequencies the values displayed in the textboxes. For the aircraft engine vibration signal Figs. 4a and 4b, acoustic signal Figs. 4d and 4e, and for the test rig with the resonance frequency in the Fig. 4c.

can be extracted if a priori knowledge about the top speed of the machine is available to isolate the IAS. For instance, the Fig. 4e shows the extracted IAS restricting the spectrogram to the frequencies constrained between 0 and 300$\mathtt{Hz}$.

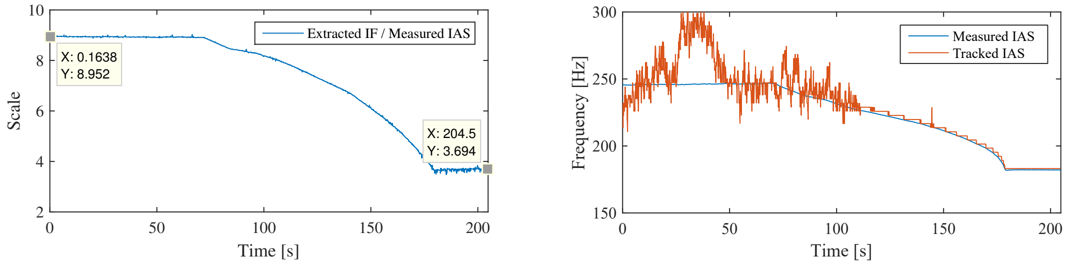

(a) Ratio $k(t) = \hat{f}_k(t)/f_0(t)$, where the measured IAS is $f_0(t)$ and the tracked IF law is $\hat{f}_k(t)$.

(b) Measured IAS in blue line and tracked IF law in red.

Figure 5 – Ratio between the 2.2$\mathtt{kHz}$ IF law and the measured IAS (left), measured IAS and extracted IAS using the spectrogram of the Fig. 4e (right).

The Fig. 5 shows the ratio between the measured IAS and the extracted 2.2$\mathtt{kHz}$ component in Fig. 5a. The aim of this figure is to show that the IF law starting at 2.2$\mathtt{kHz}$ is far from being a harmonic of the IAS. If that was the case the ratio $k(t) = \hat{f}_k(t)/f_0(t)$, should be approximately a constant real for all the t in the time domain, in contrast, the ratio $k(t)$ still shows a similar shape to the measured IAS $f_0(t)$. In contrast, the Fig. 5b shows the IAS extracted directly from the acoustic signal band-limited to the interval $[0,300]\mathtt{Hz}$, where the estimation is only accurate for the last 100$\mathtt{s}$. Alternatively, to estimate the IAS from this challenging acoustic signal, in the next Section 4.3 the IAS will be assumed to be a time-warping scale [12] rather than a particular IF law.

4.3 IAS estimation: Scale transform

In the Section 3.2 was discussed an approach based on the scale transform that does not require an initial visual inspection or to fix a set of parameters. The definition of the scale transform was introduced in the Eq. (12), but for the application of the methodology it is necessary to define an estimator. Let us consider a given phase difference $\Delta\phi_{0,i}(w)$ between the scale transform of the i-th segment and the 0-th segment, being the phase of the zero segment the phase of reference, a least squares estimation for the $\ln a_{0,i}$ is accomplished as:

$$\ln \hat{a}_{0,i} = \frac{\langle w.\Delta\phi_{0,i}(w)\rangle}{\langle w^2\rangle} \tag{15}$$

where in this case $\langle\cdot\rangle$ represents the mean value through the scales w, and $\hat{a}_{0,i}$ is an estimation for $a_{0,i}$. Last but not least, the core definition that relates the scale gap between segments to the IAS, it is the definition of the ISRF, which is noted as ΔV_i defined as follows:

$$a_{0,i} = \frac{V_i}{V_0} = 1 + \frac{V_i - V_0}{V_0} = 1 + \Delta V_i \tag{16}$$

where ΔV_i represents the speed gap between the initial 0-th segment and the i-th segment, it should be pointed out that this quantity by definition is always zero for ΔV_0.

As results, the Fig. 6 shows a test in a numerical signal built as a superposition of three sinusoid functions related in a harmonic way. Where the fundamental frequency is $f_0(t) = 60 + 5\cos(2\pi 0.25t)$, the signal is also contaminated with AWGN to achieve an SNR of 3$\mathtt{dB}$, making the signal stochastic. it should be pointed out that to use the scale transform based approach each signal segment is assumed to have a constant speed V_i, consequently, for this assumption to hold the window function should be small enough. Another restriction stated in [12] is that this methodology is not suitable for large speed variations like a run-up test, for that reason the IAS of this numerical case is a cosinusoidal function instead of the chirp of the Fig. 1a.

The Fig. 6a shows the spectrogram of the numerical signal, where as in all the preceding spectrograms, it was used a Hamming window with a duration of 0.5$\mathtt{s}$ approximately. The Fig. 6b shows the resulting ISRF and the theoretical ISRF. From the Fig. 6b is concluded that the estimated ISRF shows a remarkable accuracy for this numerical signal considering that this algorithm is entirely blind.

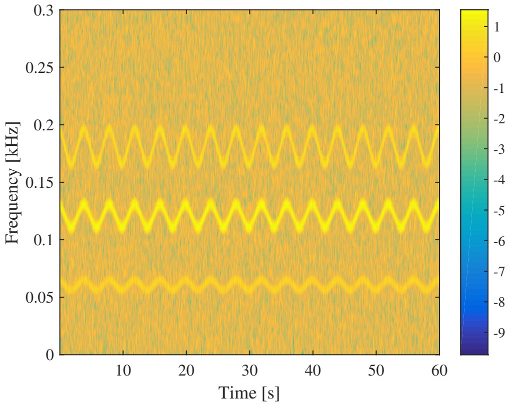

(a) Spectrogram of a numerical signal composed by three harmonics.

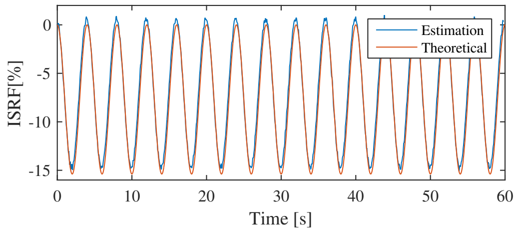

(b) ISRF obtained by means of the scale transform, and the ideal ISRF computed using the measured IAS.

Figure 6 – Spectrogram of the numerical signal (left), and its respective ISRF (right).

Due to the use of this methodology has as consequence the lost of the physical link with the original signal. To visually evaluate the performance of the obtained ISRF is mandatory to have the tachometer record to compute the ISRF of reference, as the test rig does not have this record, that signal was not taken into account in this Section 4.3. Hence, the Fig. 7 shows the results for the vibration signal in Fig. 7a and the acoustic signal in Fig. 7b both recorded from the aircraft engine.

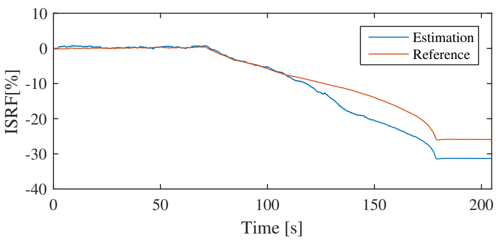

(a) Estimated ISRF for the vibration record..

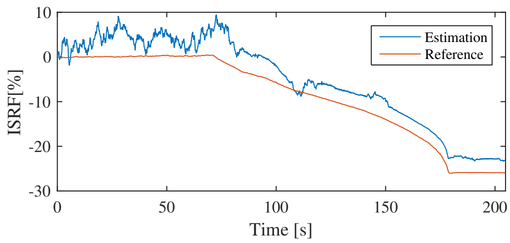

(b) Estimated ISRF for the acoustic record.

Figure 7 – Estimated ISRF (in blue), and the ISRF of reference (in red) for the vibration Fig. 7a and acoustic Fig. 7b records from the aircraft engine.

As was stated by the authors in [12] the performance of the scale transform based approach for the vibration signal decreases when large variations of the speed are present, as shown in the Fig. 7a. However, this error could also be caused by the influence of the 2.2`kHz` component, due to this technique uses all the spectral components of the signal bellow 6.25`kHz`. Even though, the interesting result is for the acoustic signal in the Fig. 7b, where the IAS and its harmonics are masked at the utmost by the harmonic family of the 2.2`kHz` component. Even in this challenging scenario the characterization using the scale transform attempts to hold but leaving room for improvement.

5 Conclusion

This paper departs with the revision of the classical definition of IF used in telecommunications, to arrive at the definition of IAS as a fundamental frequency of a harmonic sum, convolved with a transfer function, and contaminated with additive white Gaussian noise. With this definition in mind, a brief review of the state-of-the-art was introduced. The review begins with a discussion of one of the latest techniques used for multicomponent signal analysis named Empirical Mode Decomposition, arriving at parametric and nonparametric approaches for the fundamental frequency estimation.

The studied parametric techniques on the state-of-the-art are mainly based on adaptive filters, being the most popular the Kalman Filter (EKF, UKF) and the Particle Filter. Where the strongest limitation of these approaches are the modeling itself and the initialization of the parameters, nevertheless, in [6] the authors propose a divide and conquer strategy to solve the EKF above-mentioned limitations, but considering only small variations on the IAS. For the non-parametric approaches, the most interesting are the works [29, 30]. Since, they propose an alternative characterization of the IAS as a time-warping function, being this a more general approach concerning the traditional IF estimation based ones. The drawback is that; all physical link is lost, principally in [30] where the problem of IAS estimation is reformulated in terms of ISRF.

For the sake of completeness, an experimental set-up was proposed with three challenging signals, a vibration signal from a test rig, a vibration signal (publicly available), and acoustic signal both from an aircraft. The algorithm chosen as a baseline for the IAS estimation was a robust TFD based recursive algorithm. From which we can conclude that the IAS can be accurately extracted from a vibration signal. However, it will always be required previous knowledge about the machine or an elevated level of expertise for the initialization of the algorithms and/or posterior scale correction. For the acoustic signal, the accuracy of the extracted signal using the TFD based tracking must be improved. Nevertheless, this is not a trivial task due to the IAS, and its harmonics are not the dominant spectral components of the signal. A gasp of the solution was achieved applying an alternative characterization of the IAS as a time-warping function, estimating the ISRF. As future work, the authors hope that the results obtained using the acoustic signal will be improved either deeply studying the *scale domain*, either relating the 2.2kHz component to the IAS, being the second case a less general solution, due to it depends on the case of study.

Acknowledgements

The authors acknowledge “Le Programme Avenir Lyon Saint-Etienne (PALSE)” of the Université de Lyon.

References

[1] R. B. Randall, J. Antoni, *Rolling element bearing diagnostics - a tutorial*, Mechanical Systems and Signal Processing, vol. 25, no. 2 (2011), pp. 485–520.

[2] R. Zimroz, J. Urbanek, T. Barszcz, W. Bartelmus, F. Millioz, N. Martin, *Measurement of instantaneous shaft speed by advanced vibration signal processing-application to wind turbine gearbox*, Metrology and Measurement Systems, vol. 18, no. 4 (2011), pp. 701–712.

[3] Q. Leclère, H. André, J. Antoni, *A multi-order probabilistic approach for instantaneous angular speed tracking debriefing of the cmmno'14 diagnosis contest*, Mechanical Systems and Signal Processing (2016).

[4] D. Rémond, J. Antoni, R. B. Randall, *Instantaneous angular speed (ias) processing and related angular applications*, Mechanical Systems and Signal Processing, vol. 45, no. 1 (2014), pp. 24–27.

[5] J. Urbanek, T. Barszcz, R. Zimroz, J. Antoni, *Application of averaged instantaneous power spectrum for diagnostics of machinery operating under non-stationary operational conditions*, Measurement, vol. 45, no. 7 (2012), pp. 1782–1791.

[6] J.-L. Dion, C. Stephan, G. Chevallier, H. Festjens, *Tracking and removing modulated sinusoidal components: a solution based on the kurtosis and the extended kalman filter*, Mechanical Systems and Signal Processing, vol. 38, no. 2 (2013), pp. 428–439.

[7] O. Cardona-Morales, L. Avendaño, G. Castellanos-Domínguez, *Nonlinear model for condition monitoring of non-stationary vibration signals in ship driveline application*, Mechanical Systems and Signal Processing, vol. 44, no. 1-2 (2014), pp. 134–148.

[8] L. Stanković, I. Djurović, S. Stanković, M. Simeunović, S. Djukanović, M. Daković, *Instantaneous frequency in time–frequency analysis: Enhanced concepts and performance of estimation algorithms*, Digital Signal Processing, vol. 35 (2014), pp. 1–13.

[9] B. Boashash, *Estimating and interpreting the instantaneous frequency of a signal. i. fundamentals*, Proceedings of the IEEE, vol. 80, no. 4 (1992), pp. 520–538.

[10] B. Boashash, *Estimating and interpreting the instantaneous frequency of a signal. ii. algorithms and applications*, Proceedings of the IEEE, vol. 80, no. 4 (1992), pp. 540–568.

[11] J. Antoni, J. Griffaton, H. André, L. D. Avendaño-Valencia, F. Bonnardot, O. Cardona-Morales, G. Castellanos-Dominguez, A. P. Daga, Q. Leclère, C. M. Vicuña, et al., *Feedback on the surveillance 8 challenge: Vibration-based diagnosis of a safran aircraft engine*, Mechanical Systems and Signal Processing (2017).

[12] F. Combet, R. Zimroz, *A new method for the estimation of the instantaneous speed relative fluctuation in a vibration signal based on the short time scale transform*, Mechanical Systems and Signal Processing, vol. 23, no. 4 (2009), pp. 1382–1397.

[13] B. Picinbono, *On instantaneous amplitude and phase of signals*, IEEE Transactions on signal processing, vol. 45, no. 3 (1997), pp. 552–560.

[14] N. E. Huang, Z. Wu, S. R. Long, K. C. Arnold, X. Chen, K. Blank, *On instantaneous frequency*, Advances in adaptive data analysis, vol. 1, no. 02 (2009), pp. 177–229.

[15] O. Cardona-Morales, E. Sierra-Alonso, G. Castellanos-Dominguez, *Blind extraction of instantaneous frequency for order tracking in rotating machines under non-stationary operating conditions*, in *Advances in Condition Monitoring of Machinery in Non-Stationary Operations*, Springer International Publishing (2016), pp. 99–110.

[16] N. E. Huang, Z. Shen, S. R. Long, M. C. Wu, H. H. Shih, Q. Zheng, N.-C. Yen, C. C. Tung, H. H. Liu, *The empirical mode decomposition and the hilbert spectrum for nonlinear and non-stationary time series analysis*, in *Proceedings of the Royal Society of London A: Mathematical, Physical and Engineering Sciences*, vol. 454, The Royal Society (1998), pp. 903–995.

[17] Y. Lei, J. Lin, Z. He, M. J. Zuo, *A review on empirical mode decomposition in fault diagnosis of rotating machinery*, Mechanical Systems and Signal Processing, vol. 35, no. 1 (2013), pp. 108–126.

[18] P. Flandrin, G. Rilling, P. Goncalves, *Empirical mode decomposition as a filter bank*, IEEE signal processing letters, vol. 11, no. 2 (2004), pp. 112–114.

[19] G. Rilling, P. Flandrin, *One or two frequencies? the empirical mode decomposition answers*, IEEE transactions on signal processing, vol. 56, no. 1 (2008), pp. 85–95.

[20] I. Daubechies, J. Lu, H.-T. Wu, *Synchrosqueezed wavelet transforms: An empirical mode decomposition-like tool*, Applied and computational harmonic analysis, vol. 30, no. 2 (2011), pp. 243–261.

[21] C. Li, M. Liang, *Time–frequency signal analysis for gearbox fault diagnosis using a generalized synchrosqueezing transform*, Mechanical Systems and Signal Processing, vol. 26 (2012), pp. 205–217.

[22] W. Yang, P. J. Tavner, W. Tian, *Wind turbine condition monitoring based on an improved spline-kernelled chirplet transform*, IEEE Transactions on Industrial Electronics, vol. 62, no. 10 (2015), pp. 6565–6574.

[23] Y. Yang, W. Zhang, Z. Peng, G. Meng, *Multicomponent signal analysis based on polynomial chirplet transform*, IEEE Transactions on Industrial Electronics, vol. 60, no. 9 (2013), pp. 3948–3956.

[24] L. Stankovic, S. Djukanovic, *Order adaptive local polynomial ft based interference rejection in spread spectrum communication systems*, IEEE Transactions on Instrumentation and measurement, vol. 54, no. 6 (2005), pp. 2156–2162.

[25] X. Li, G. Bi, S. Stankovic, A. M. Zoubir, *Local polynomial fourier transform: A review on recent developments and applications*, Signal Processing, vol. 91, no. 6 (2011), pp. 1370–1393.

[26] R. G. Brown, P. Y. Hwang, *Introduction to random signals and applied kalman filtering: with matlab exercises and solutions*, Introduction to random signals and applied Kalman filtering: with MATLAB exercises and solutions, by Brown, Robert Grover.; Hwang, Patrick YC New York: Wiley, c1997. (1997).

[27] H. Hajimolahoseini, R. Amirfattahi, H. Soltanian-Zadeh, S. Gazor, *Instantaneous fundamental frequency estimation of non-stationary periodic signals using non-linear recursive filters*, IET Signal Processing, vol. 9, no. 2 (2015), pp. 143–153.

[28] O. Cardona-Morales, L. Avendaño, G. Castellanos-Domínguez, *Nonlinear model for condition monitoring of non-stationary vibration signals in ship driveline application*, Mechanical Systems and Signal Processing, vol. 44, no. 1 (2014), pp. 134–148.

[29] H. Omer, B. Torrésani, *Time-frequency and time-scale analysis of deformed stationary processes, with application to non-stationary sound modeling*, Applied and Computational Harmonic Analysis (2015).

[30] F. Combet, P. Jaussaud, N. Martin, *Estimation of slight speed gaps between signals via the scale transform*, Mechanical systems and signal processing, vol. 19, no. 2 (2005), pp. 239–257.